

Phonons, pions and quasi-long-range order in spatially modulated chiral condensates

Yoshimasa Hidaka,¹ Kazuhiko Kamikado,¹ Takuya Kanazawa,² and Toshifumi Noumi¹

¹*Theoretical Research Division, Nishina Center, RIKEN, Wako, Saitama 351-0198, Japan*

²*iTHES Research Group and Quantum Hadron Physics Laboratory, RIKEN, Wako, Saitama 351-0198, Japan*

We investigate low-energy fluctuations in the real kink crystal phase of dense quark matter within the Nambu–Jona-Lasinio model. The modulated chiral condensate breaks both the translational symmetry and chiral symmetry spontaneously, which leads to the appearance of phonons and pions that are dominant degrees of freedom in the infrared. Using the Ginzburg–Landau expansion near the Lifshitz point, we derive elastic free energies for phonons and pions in dependence on the temperature and chemical potential. We show that the one-dimensional modulation is destroyed by thermal fluctuations of phonons at nonzero temperature and compute the exponent that characterizes the anisotropic algebraic decay of quasicondensate correlations at long distance. We also estimate finite-volume effects on the stability of the real kink crystal and briefly discuss the possibility of its existence in neutron stars.

I. INTRODUCTION

Revealing the nature of QCD at finite temperature and baryon density has been one of the most important challenges in high-energy physics. At low temperature and low baryon chemical potential, the ground state of QCD is characterized by chiral symmetry breaking and color confinement. Under extreme conditions, QCD is known to exhibit novel phenomena, such as deconfinement of color degrees of freedom at high temperature and color superconductivity at high baryon density. These areas are extensively investigated; see [1–3] for reviews.

Inhomogeneous phases in QCD have been studied for a long time. Pivotal examples include p -wave pion condensation in nuclear matter [4], a chiral density wave at large N_c [5–9] and crystalline color superconductivity at high density [10, 11], in close analogy to the Fulde–Ferrell–Larkin–Ovchinnikov (FFLO) phases of superconductivity [12, 13]. Recently, an exotic phase of dense quark matter in which the chiral condensate forms a spatial soliton lattice has attracted considerable attention [14–19], as reviewed in [20]. Initially, a theoretical breakthrough was made in the study of inhomogeneous chiral condensation in (1+1)-dimensional field theories [21]. A general complex kink solution to the Ginzburg–Landau (GL) equation for the chiral Gross–Neveu model was then discovered [22, 23] and its relevance in the phase diagram of the (chiral) Gross–Neveu model was elucidated [24]. The issue of inhomogeneous condensation in (3+1)-dimensional theories was revisited by Nickel [15] who introduced a novel technique for applying the general solution of the Gross–Neveu model to the Nambu–Jona-Lasinio (NJL) model and thereby pointed out the emergence of a one-dimensionally periodic chiral condensate in the vicinity of the first-order chiral transition line that appears when limiting to a homogeneous condensate. Considering that higher-dimensional modulations are energetically disfavored against one-dimensional modulations [17, 18], there is a high chance that one-dimensionally modulated chiral condensates may indeed be the ground state of QCD in a certain range of temperature and chemical potential.

So far almost all studies on the inhomogeneous chiral condensation have been limited to the mean-field approximation and inclusion of collective fluctuations of the order parameter is an urgent issue. It has been well known since Landau’s seminal work in the 1930s that in three dimensions a one-dimensional spatial order is unstable against thermal fluctuations. This is known as the Landau–Peierls theorem [25, 26]. The destabilized long-range order leaves its imprint in the power-law decay of the order parameter, characteristic of a phase with quasi-long-range order. This is reminiscent of two-dimensional systems with continuous symmetry, in which a long-range order is prohibited [27, 28] and the Berezinskii–Kosterlitz–Thouless phase emerges at low temperature [29, 30].

In this paper, we elucidate various properties of gapless excitations on a spatially modulated chiral condensate in the NJL model. Our analysis is based on the 6th-order GL expansion of the NJL model near the critical point, for which an analytical solution to the GL equation, called the *real kink crystal* [22–24], is available. Because the kink crystal breaks both the translational symmetry along one axis and chiral symmetry, we encounter smectic phonons in addition to ordinary pions. We will derive the elastic free energy of these modes and reveal how they modify the mean-field picture of this phase. While the analysis presented here closely parallels preceding works about fluctuations in liquid crystals [31–33] and in the FFLO phases of fermionic superfluids [34–39], our analysis has a specific focus on quantitative understanding of those gapless modes in the context of dense QCD.

The outline of this paper is as follows. In Sec. II, we develop a general argument for low-energy fluctuations over a one-dimensionally modulated order parameter. In Sec. III, the GL-expanded NJL model is analyzed. We first derive the free energy for the translational phonon mode and argue that thermal fluctuations of phonons wash out the modulated condensate and lead to a phase with quasi-long-range order. Next we derive the free energy of pions. Finally, Sec. IV is devoted to concluding remarks. Some technicalities are summarized in the Ap-

pendixes.

II. SYMMETRY CONSIDERATION

When a chiral condensate is modulated along one dimension, the phonon mode (u) appears as the Nambu–Goldstone (NG) mode of translational symmetry breaking, in addition to pions (π). In the real kink crystal phase discussed later, the vectorial isospin symmetry $SU(2)_V$ is unbroken and there is no mixing between phonons and pions. Therefore, the symmetry breaking pattern reads¹

$$\mathbf{R}^3 \rtimes \text{SO}(3) \rightarrow [\mathbf{R}^2 \rtimes \text{SO}(2)] \times [\text{discrete symmetry}] \quad (1)$$

in addition to the chiral symmetry breaking pattern, $SU(2)_R \times SU(2)_L \rightarrow SU(2)_V$. Here \mathbf{R}^d and $\text{SO}(d)$ denote the d -dimensional translational and rotational symmetry groups, respectively. The discrete symmetry includes a discrete translational symmetry along the modulated direction of the condensate as a subgroup, which is a remnant of the translation \mathbf{R} in this direction. Other elements of the discrete group depend on the shape of the kink crystal².

In this symmetry breaking pattern, two rotational and one translational symmetries are spontaneously broken. We note that there appears no gapless mode associated with the broken rotational symmetry. In general, the number of NG modes does not coincide with that of broken global spacetime symmetries [40–42].

In the remainder of this section, we present a general discussion on the effective low-energy theory of phonons (see also [25, 31, 32, 43, 44]). Let us consider a theory with the free energy $F[\phi] = \int d^3x \mathcal{F}(\phi, \partial\phi)$ and assume that $\langle \phi \rangle = \phi_0(\mathbf{x})$ is a static solution minimizing $F[\phi]$. In the following, we assume that the free energy density \mathcal{F} respects rotational and translational symmetries. If ϕ_0 is modulated in one direction and is homogeneous in the transverse directions, one can write it as $\phi_0(\mathbf{x}) \propto f(\mathbf{q} \cdot \mathbf{x})$, where \mathbf{q} is a vector parallel to the modulated direction and $f(\cdot)$ is a dimensionless function. Now we consider a translational fluctuation corresponding to the phonon around this solution, $\phi(\mathbf{x}) \propto f(\mathbf{q} \cdot \mathbf{x} + qu(\mathbf{x}))$ with $q = |\mathbf{q}|$. Plugging this function into $F[\phi]$ and expanding in powers of u and ∇u , one obtains the effective theory for the u field.

Rotational symmetry of the original free energy implies that $f(\mathbf{q} \cdot \mathbf{x})$ and $f(\mathbf{q}' \cdot \mathbf{x})$, with a rotated vector \mathbf{q}' , have the same value of $F[\phi]$. Writing $\mathbf{q}' \cdot \mathbf{x} = \mathbf{q} \cdot \mathbf{x} + (\mathbf{q}' - \mathbf{q}) \cdot \mathbf{x}$, it follows that the fluctuation $qu(\mathbf{x}) = (\mathbf{q}' - \mathbf{q}) \cdot \mathbf{x}$ does not cost any additional free energy. This imposes a constraint on the form of the effective theory. Suppose \mathbf{q} points in the z direction, with no loss of generality. Under a rotation by θ about the y axis, the gradients of u are given by

$$\partial_z u = -1 + \cos \theta, \quad \partial_x u = \sin \theta, \quad (2)$$

hence $(1 + \partial_z u)^2 + (\nabla_{\perp} u)^2$ is invariant under the rotation. Then the effective theory of u invariant under rotation can be constructed as a function of $(1 + \partial_z u)^2 + (\nabla_{\perp} u)^2 = 2\partial_z u + (\nabla u)^2 + 1$ and higher-order derivative terms such as $\nabla_{\perp}^2 u$.

A total derivative term $\partial_z u$ would be allowed in the effective theory if we only require the stationary condition for F under a variation of ϕ with fixed boundary conditions. However, global minimization of F excludes this term, which can be seen as follows. Consider a fluctuation $u = \varepsilon z$ over the ground state $\phi_0(z)$. It corresponds to a dilatation $z \rightarrow (1 + \varepsilon)z$. In the presence of a term $\propto A\partial_z u$ in \mathcal{F} , this u will generate an energy shift

$$\Delta \mathcal{F} = \varepsilon A + \mathcal{O}(\varepsilon^2), \quad (3)$$

indicating that there exists a lower-energy direction when $A \neq 0$. In other words, we have $A = 0$ when the condensate is the ground state.

This observation imposes a constraint that \mathcal{F} should depend on $2\partial_z u + (\nabla u)^2$ at least quadratically. Thus we conclude that the free energy density for the phonon assumes a form

$$\mathcal{F} = B \left[\partial_z u + \frac{1}{2}(\nabla u)^2 \right]^2 + C(\nabla_{\perp}^2 u)^2, \quad (4)$$

at the leading order of the derivative expansion, with low-energy constants B and C . In deriving (4) we exploited the fact that the term $(\partial_z u)(\nabla_{\perp}^2 u)$ is prohibited if we assume parity invariance at low energy (see Appendix E3 for more details). Here we emphasize that the absence of $(\nabla_{\perp} u)^2$ in \mathcal{F} makes the dispersion of u strongly anisotropic.

Such an anisotropic dispersion does not appear when the rotational symmetry is *explicitly* broken, just as in QCD under external magnetic fields. This is shown in Appendix A.

III. REAL KINK CRYSTAL

In this section, we study the long-wavelength fluctuations of the real kink crystal chiral condensate within the NJL model in the chiral limit. The real kink crystal is known to be energetically favored over a spatially homogeneous chiral condensate in a certain range of temperature and chemical potential [15]. We analyze the GL

¹ The free energy has no Lorentz symmetry because it is broken by the existence of matter. Therefore, we do not take into account the Lorentz symmetry breaking as the breaking pattern.

² In general, real kink crystals can be classified by the Frieze group. The real kink crystal discussed in this paper has the $\mathbb{Z} \rtimes \mathbb{Z}_2$ symmetry, where \mathbb{Z} and \mathbb{Z}_2 represent the glide reflection symmetry and the reflection symmetry at a certain vertical line, respectively.

free energy of the NJL model near the Lifshitz point and derive the elastic free energy of phonons and pions on the kink crystal on the basis of Bloch's theorem for particles moving in a periodic potential. For simplicity we will not consider dynamical aspects of those fluctuations and also ignore gapped fluctuations.

A. Phase diagram

According to Nickel's work [14], the GL expansion for the (3+1)-dimensional NJL model in the chiral limit, to sixth order, reads

$$\begin{aligned} \Omega_{\text{GL}}[M(\mathbf{x})] = & \alpha_2 M^2 + \alpha_4 \{M^4 + (\nabla M)^2\} \\ & + \alpha_6 \{2M^6 + 10M^2(\nabla M)^2 + (\Delta M)^2\}. \end{aligned} \quad (5)$$

Here the real-valued field $M(\mathbf{x})$ represents the chiral condensate. For simplicity, the pionic condensates $\langle \bar{\psi} i \gamma_5 \tau^a \psi \rangle$ are suppressed at this stage. The neutral pion fluctuation will be later incorporated in Sec. III D, and a fully isospin-symmetric form of the GL expansion is presented in Appendix B.

The coefficients in the GL expansion (5) are given as functions of temperature (T) and chemical potential (μ) [14]

$$\begin{aligned} \alpha_2 = & \frac{\alpha'_2}{2} + \frac{1}{4G}, \quad \alpha_4 = \frac{\alpha'_4}{4}, \quad \alpha_6 = \frac{\alpha'_6}{12}, \\ \alpha'_n \equiv & (-1)^{\frac{n}{2}} 4N_c N_f T \sum_n \int_{\text{reg}} \frac{d^3 p}{(2\pi)^3} \frac{1}{[(\omega_n + i\mu)^2 + p^2]^{n/2}}, \end{aligned} \quad (6)$$

where G is the four-fermion coupling in the NJL model and N_c and N_f are the numbers of colors and flavors, respectively. The momentum integrals for α'_2 and α'_4 are ultraviolet divergent and must be regularized with some regularization scheme. This GL expansion is valid near the QCD critical point at which $\alpha_2 = \alpha_4 = 0$. We require $\alpha_6 > 0$ for stability.

To find the correct ground state of the GL free energy, we have to solve the GL equation:

$$\frac{\delta}{\delta M(\mathbf{x})} \int d^3 y \Omega_{\text{GL}}[M(\mathbf{y})] = 0. \quad (7)$$

If we assume a one-dimensional modulation in the z direction, the GL equation reduces to that of the GN₂ model, which has a family of solutions [22–24] given by

$$M_0(z) = q\sqrt{\nu} \text{sn}(qz; \nu), \quad (8)$$

where q is a function of ν through the relation

$$q^4 + \frac{\nu + 1}{\nu^2 + 4\nu + 1} \frac{\alpha_4}{\alpha_6} q^2 + \frac{1}{\nu^2 + 4\nu + 1} \frac{\alpha_2}{\alpha_6} = 0. \quad (9)$$

One can easily check that M_0 with (9) satisfies the GL equation (7).³ The elliptic parameter $\nu \in [0, 1]$ is not determined by the GL equation alone and must be fixed from the requirement of lowest energy per period. ν controls the shape of the solution; $\text{sn}(z; 0) = \sin z$ and $\text{sn}(z; 1) = \tanh z$. We can identify the solution $\text{sn}(z; 1)$ as the homogeneous solution because thermodynamically $\tanh z$ is equivalent to a spatially homogeneous configuration. Let L be the period of M_0 and Q the wave number of M_0 , respectively given by

$$L \equiv \frac{4\mathbf{K}(\nu)}{q} \quad \text{and} \quad Q \equiv \frac{2\pi}{L}, \quad (10)$$

where $\mathbf{K}(\nu) \equiv \int_0^{\pi/2} dt (1 - \nu \sin^2 t)^{-1/2}$ is the complete elliptic integral of the first kind. In what follows, we denote the average of a periodic function as

$$\oint F \equiv \frac{1}{L} \int_0^L dz F(z). \quad (11)$$

To map out the phase diagram near the tricritical point, we need to evaluate (6) for given T and μ . In this work, the Matsubara sum in (6) was done analytically, whereas the momentum integral was regularized by a three-momentum cutoff Λ . (See Appendix C for additional comments on the choice of regularization.) In this work, we have used the parameter set in [46]: $\Lambda = 632$ MeV and $G\Lambda^2 = 2.173$. The value of ν at a given (T, μ) was numerically determined through minimization of the GL free energy per period

$$\oint \Omega_{\text{GL}}[M_0(z)]. \quad (12)$$

Then q immediately follows from ν via (9).

In Fig. 1, we show the resulting phase diagram of the GL-expanded NJL model (5). Strictly speaking, the GL analysis is only valid in a region with a small order parameter and small spatial variation, so the phase structure shown here is only intended to be a qualitative guide. In the red region, the kink crystal chiral condensate ($0 < \nu < 1$) is energetically favored, while in the green region, the homogeneous chiral condensate ($\nu = 1$) develops. The three phases (real kink crystal, homogeneous and symmetric phases) meet at the Lifshitz point, $(T, \mu) = (81.4, 276.4)$, at which $\alpha_2 = \alpha_4 = 0$. The real kink crystal phase is very narrow near the Lifshitz point and is almost invisible in the plot. The phase structure from our numerical calculation is consistent with analyses with a non-expanded effective potential [15] except

³ The most general solution to (7) is given by a quasi-periodic function written by the Riemann theta function with genus $g = 3$ [45], which is considerably more complicated than the elliptic function, (8). In the following, we assume that (8) is energetically favored over higher genus functions, and leave a more comprehensive analysis to future work. We thank D. A. Takahashi for useful comments on this point.

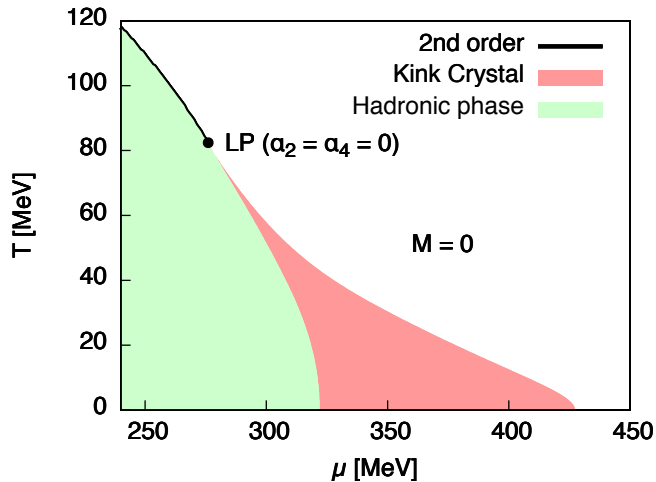


FIG. 1. Phase diagram of the NJL model in the chiral limit with 6th order GL expansion. The Lifshitz point is located at $(T, \mu) = (81.4, 276.4)$ [MeV].

that the real kink crystal phase in Fig. 1 appears to be broader at low temperature. The phase boundary in our results are consistent with Nickel's observation [14] that the real kink crystal phase is favored if $\alpha_2 > 0$ and

$$-\sqrt{\frac{54}{5}\alpha_2\alpha_6} < \alpha_4 < -2\sqrt{\alpha_2\alpha_6}. \quad (13)$$

In Fig. 2, we plot the root-mean-square condensate

$$\langle\langle M_0^2 \rangle\rangle^{1/2} \equiv \sqrt{\oint M_0(z)^2} \quad (14)$$

and the wave number Q of the real kink crystal at $T = 70$ MeV and $T = 10$ MeV. It is observed that both phase transitions (from the kink crystal phase to the homogeneous and to the symmetric phase) are of second order: At the transition with lower μ , the wave number gradually rises from zero, implying the formation of widely separated domain walls. On the other hand, at the transition with higher μ , the amplitude of M vanishes smoothly with keeping a nonzero wave number. This behavior is consistent with the preceding work with a non-expanded potential [15].

B. Phonons

We would like to derive the elastic free energy of phonons originating from the spontaneous breaking of translation symmetry in the real kink crystal phase. Let us substitute

$$\begin{aligned} M(\mathbf{x}) &= M_0(z + u(\mathbf{x})) \\ &= M_0(z) + M_0'(z)u(\mathbf{x}) + \frac{1}{2}M_0''(z)u(\mathbf{x})^2 + \dots \end{aligned}$$

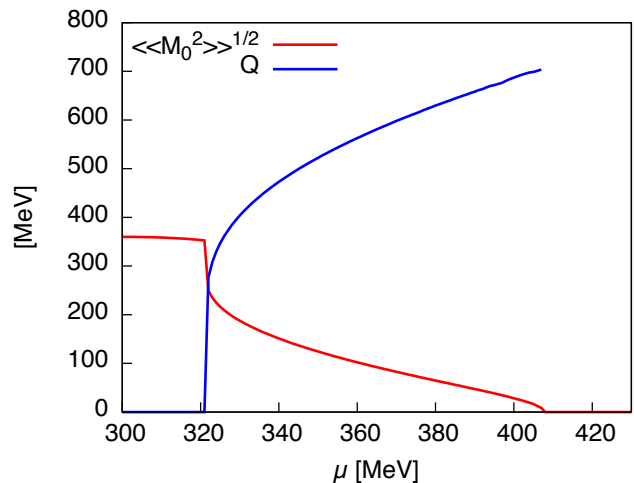
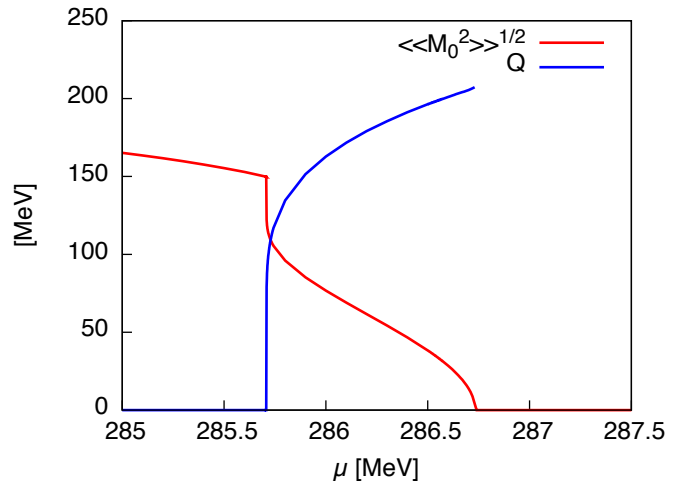


FIG. 2. The average magnitude of M and its wave number Q , at $T = 70$ MeV (**top**) and $T = 10$ MeV (**bottom**).

into (5) and expand in u , dropping total derivatives. Then

$$\begin{aligned} \Omega_{\text{GL}}[M(\mathbf{x})] &= \Omega_{\text{GL}}[M_0(z)] + \frac{f_1(z)}{2}(\partial_z u)^2 + \frac{f_2(z)}{2}(\partial_z^2 u)^2 \\ &+ \frac{g_1(z)}{2}(\nabla_{\perp} u)^2 + \frac{g_2(z)}{2}(\nabla_{\perp}^2 u)^2 \\ &+ h_1(z)(\partial_z u)(\nabla_{\perp}^2 u) \\ &+ h_2(z)(\partial_z^2 u)(\nabla_{\perp}^2 u) + \mathcal{O}(u^3), \end{aligned} \quad (15)$$

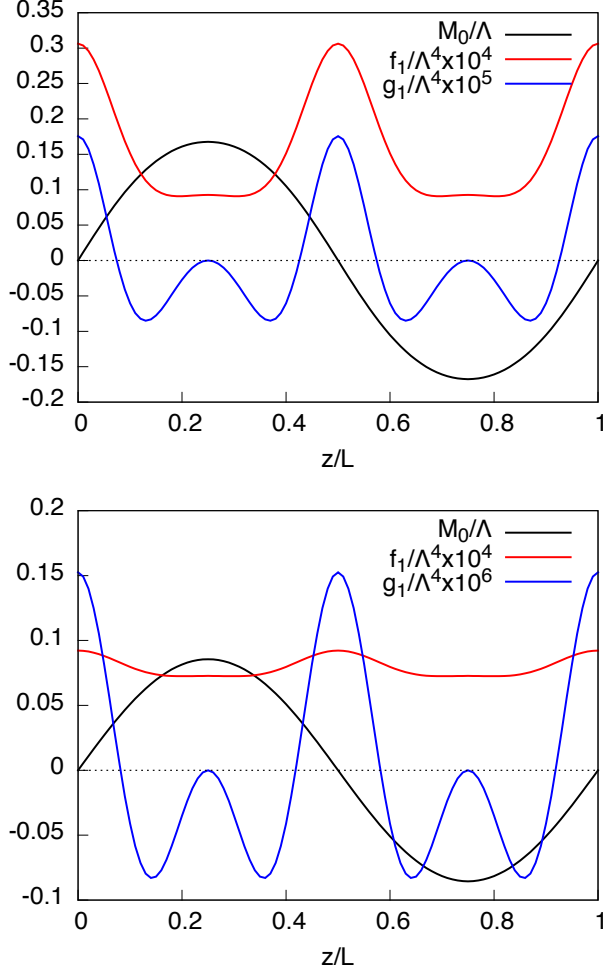


FIG. 3. The order parameter M_0 and the coefficient functions f_1 and g_1 over one period at $(T, \mu) = (70, 286.0)$ [MeV] (**top**) and $(T, \mu) = (70, 286.5)$ [MeV] (**bottom**). All functions are measured in units of Λ . The period L is 7.71 fm (**top**) and 6.40 fm (**bottom**), respectively.

where $\nabla_{\perp} \equiv (\partial_x, \partial_y)$ is a transverse derivative and $f_1, f_2, g_1, g_2, h_1, h_2$ are defined as

$$\begin{aligned}
 f_1(z) &= 2(\alpha_4 + 10\alpha_6 M_0^2)(M_0')^2 \\
 &\quad + 4\alpha_6 \{ (M_0'')^2 - 2M_0' M_0'''\}, \\
 f_2(z) &= 2\alpha_6 (M_0')^2, \\
 g_1(z) &= 2(\alpha_4 + 10\alpha_6 M_0^2)(M_0')^2 - 4\alpha_6 M_0' M_0''', \\
 g_2(z) &= 2\alpha_6 (M_0')^2, \\
 h_1(z) &= 4\alpha_6 M_0' M_0'', \quad h_2(z) = 2\alpha_6 (M_0')^2.
 \end{aligned} \tag{16}$$

Figure 3 displays the order parameter and some of the coefficient functions at $(T, \mu) = (70, 286.0)$ [MeV] and $(T, \mu) = (70, 286.5)$ [MeV]. Obviously the functions share the same period with the order parameter. Note that $(\nabla_{\perp} u)^2$ is present in (15) even though the general theory in Sec. II suggests that this term should be absent in the effective action of low-energy modes. This is not a con-

tradiction: since the expansion (15) includes functions f_1, g_1 , etc., that vary over the microscopic length scale L , we cannot immediately infer the dispersion of modes with wavelength much longer than L from there.

As emphasized in Sec. II the free energy of a modulated condensate must be invariant under a spatial rotation. This can be checked for (15) as follows. An infinitesimal rotation about y axis is equivalent to a displacement field $u(\mathbf{x}) = -\sin\theta x + (1 - \cos\theta)z$ with $|\theta| \ll 1$. Plugging this into (15) and expanding in θ , we find the leading term to be $\frac{1}{2}g_1(z)\theta^2$. Then, for the rotational symmetry to be preserved, the average of g_1 must vanish:

$$\oint g_1(z) = 0. \tag{17}$$

A direct proof of this equality based on the minimization of energy is given in Appendix D for completeness. We remark that (17) is not automatically ensured by the GL equation (7) [or equivalently (9)] alone—we must minimize the energy per period, to have (17) satisfied. It will be shown below that the property (17) is instrumental in making the dispersion of phonons anisotropic, in accordance with the general argument in Sec. II.

To evaluate the low-energy phonon fluctuation on the real kink crystal, let us consider the eigenvalue equation

$$Eu = \frac{\delta F[u]}{\delta u} \tag{18}$$

with

$$\begin{aligned}
 F[u] &\equiv \int d^3x \left[\frac{f_1(z)}{2} (\partial_z u)^2 + \frac{f_2(z)}{2} (\partial_z^2 u)^2 \right. \\
 &\quad + \frac{g_1(z)}{2} (\nabla_{\perp} u)^2 + \frac{g_2(z)}{2} (\nabla_{\perp}^2 u)^2 \\
 &\quad \left. + h_1(z) (\partial_z u) (\nabla_{\perp}^2 u) + h_2(z) (\partial_z^2 u) (\nabla_{\perp}^2 u) \right].
 \end{aligned} \tag{19}$$

The eigenvalue equation in the explicit form reads

$$H_u u = Eu \tag{20}$$

with

$$\begin{aligned}
 H_u &\equiv -\partial_z (f_1 \partial_z) + \partial_z^2 (f_2 \partial_z^2) - g_1 \nabla_{\perp}^2 + g_2 \nabla_{\perp}^4 \\
 &\quad - (\partial_z h_1) \nabla_{\perp}^2 + \nabla_{\perp}^2 \{h_2, \partial_z^2\}_+,
 \end{aligned} \tag{21}$$

where $\{ \}_+$ denotes the anti-commutation relation and $\{h_2, \partial_z^2\}_+ u = h_2 \partial_z^2 u + \partial_z^2 (h_2 u)$. As the operator H_u acting on u is real and Hermitian, the eigenvalue E is real, and we can elevate u to a complex-valued function without changing the eigenvalues. We note that E itself does not give the dispersion relation of the phonon, but is rather related to the phonon susceptibility. The dispersion relation can in principle be obtained from the time evolution equation, but it is complicated because of the mixing with hydrodynamic modes (see, e.g., [32]) and will not be discussed further in this paper.

Since all the coefficient functions are periodic functions sharing the same period, it follows from Bloch's theorem

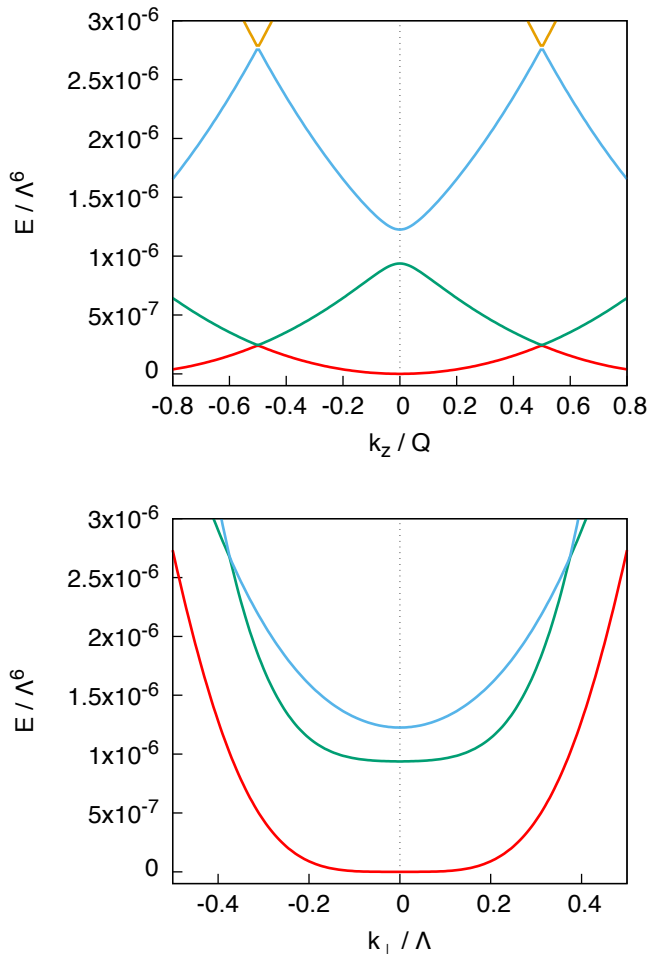


FIG. 4. Eigenvalues of H_u in (21) at $(T, \mu) = (70, 286.0)$ [MeV], for $k_{\perp} = 0$ (top) and for $k_z = 0$ (bottom). The domain $-0.5 \leq k_z/Q \leq 0.5$ is the first Brillouin zone. k_z and E are normalized by Q , and k_{\perp} is normalized by the UV cutoff scale Λ .

that u can be decomposed into a plane wave and a periodic function,

$$u(\mathbf{x}) = e^{i\mathbf{k}_{\perp} \cdot \mathbf{x}_{\perp}} e^{ik_z z} \phi(z), \quad (22)$$

where k_{\perp} is the momentum in transverse directions, k_z is the so-called *crystal momentum*, and $\phi(z)$ is a periodic function, viz. $\phi(z + L) = \phi(z)$. Substituting (22) into (20) yields an eigenvalue equation for ϕ , which we have solved numerically by way of a Fourier decomposition $\phi(z) = \sum_{n=-n_{\max}}^{n_{\max}} \phi_n e^{inQz} / \sqrt{L}$ with $n_{\max} = 20$. To see convergence, we have increased n_{\max} up to 30 and confirmed that the results are unchanged.

In Fig. 4, we show the eigenvalue E numerically computed for varying k_z and k_{\perp} . A marked difference from the eigenvalue of particles in a free space is that there are *infinitely many* levels for given momenta, in analogy to electrons in metals which develop a band structure.

It is the lowest eigenvalue E_0 (red curves in Fig. 4) that

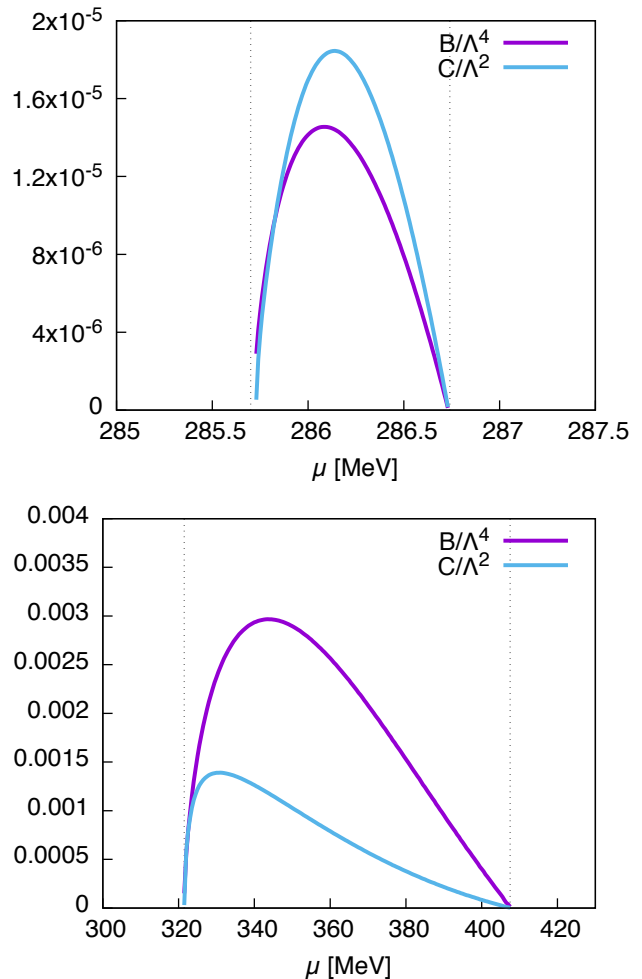


FIG. 5. B and C at $T = 70$ MeV (top) and $T = 10$ MeV (bottom). B and C are normalized by the UV cutoff parameter Λ with appropriate dimensions. The dotted vertical lines mark the boundaries of the modulated phase.

pertains to the free energy of long-wavelength phonons. By adopting a variational approach, one can rigorously show that E_0 behaves for $k_z \sim k_{\perp} \sim 0$ as

$$E_0 \sim Bk_z^2 + Ck_{\perp}^4, \quad (23)$$

where B and C are functions of T and μ . The absence of the $\mathcal{O}(k_{\perp}^2)$ term in (23) is guaranteed by the property (17). The proof of (23) is somewhat technical and is relegated to Appendix E. Equation (23) shows that the elastic free energy of low-energy phonons becomes

$$F_{\text{el}}^u = \frac{1}{2} \int d^3x [B(\partial_z u)^2 + C(\nabla_{\perp}^2 u)^2]. \quad (24)$$

One may suspect that the coefficient B would be given by $\mathcal{f} f_1$. However, as shown in Appendix E, this naive guess is incorrect; the coupling between ϕ_0 and $\phi_{n \neq 0}$ is not negligible even in the perturbation series in k_z .

To extract the values of B and C from eigenvalues, we have numerically fitted the curve of E_0 with trial func-

tions $E_0 = Bk_z^2$ and $E_0 = Ck_\perp^4$, respectively, with B and C treated as fitting parameters. Figure 5 shows B and C at $T = 70$ MeV and $T = 10$ MeV obtained this way. Notably, B and C in Fig. 5 are positive throughout the real kink crystal phase, which proves local stability of this condensate in agreement with numerical results in [17]. Because the phonon mode exists only in the real kink crystal phase, it is natural that both coefficients tend to zero at the phase boundaries, although the eigenvalues E were too small near the left boundary for $T = 70$ MeV to perform a reliable fitting.

We mention that the spectrum of gapless excitations over the same background (8) has also been worked out in [45] with entirely different methods. However a direct comparison is difficult owing to the fact that the model in [45] is non-relativistic and in one space dimension, while our model is relativistic and in three space dimensions.

C. IR divergence and quasi-long-range order

Next, we wish to evaluate the impact of thermal fluctuations of phonons on the stability of the real kink crystal. Taking the Fourier decomposition $M(\mathbf{x}) = \sum_n \mathcal{M}_n e^{inQ(z+u(\mathbf{x}))} / \sqrt{L}$, treating u in the Gaussian approximation and ignoring the pion fluctuation, we obtain

$$\begin{aligned} \langle M(\mathbf{x}) \rangle &= \frac{1}{\sqrt{L}} \sum_n \mathcal{M}_n \langle e^{inQ(z+u(\mathbf{x}))} \rangle \\ &= \frac{1}{\sqrt{L}} \sum_n \mathcal{M}_n e^{inQz} \exp \left[-\frac{1}{2} n^2 Q^2 \langle u^2 \rangle \right] \end{aligned} \quad (25)$$

with

$$\begin{aligned} \langle u^2 \rangle &= \frac{2\pi}{(2\pi)^3} \int_{\ell_\perp^{-1}}^\Lambda dk_\perp k_\perp \int_{-\Lambda}^\Lambda dk_z \frac{T}{Bk_z^2 + Ck_\perp^4} \\ &\sim \frac{T}{4\pi\sqrt{BC}} \log \frac{\ell_\perp}{\sqrt{C/B}}, \end{aligned} \quad (26)$$

where we have only incorporated the lowest Matsubara mode since it is dominant in the infrared. The momentum integral is IR divergent and is regularized by a cutoff ℓ_\perp . One can regard ℓ_\perp as the transverse diameter of the quark matter in a compact star. In the thermodynamic limit $\ell_\perp \rightarrow \infty$, the condensate (25) drops to zero with negative powers of ℓ_\perp , implying that the one-dimensional modulation is wiped out by thermal fluctuations at any low $T > 0$, a phenomenon known as the Landau-Peierls instability. In fact, if the average amplitude of displacement fluctuation exceeds the interval of layers, it does not make sense to speak of a spatial long-range order. We emphasize that this instability persists even at nonzero quark masses, since it originates from phonons that remain elastic regardless of the quark masses.

In the thermodynamic limit, the system instead exhibits a *quasi-long-range order*. Expanding M in Fourier series and ignoring non-Gaussian effects and pion fluctuations, we find that the correlation function of the order

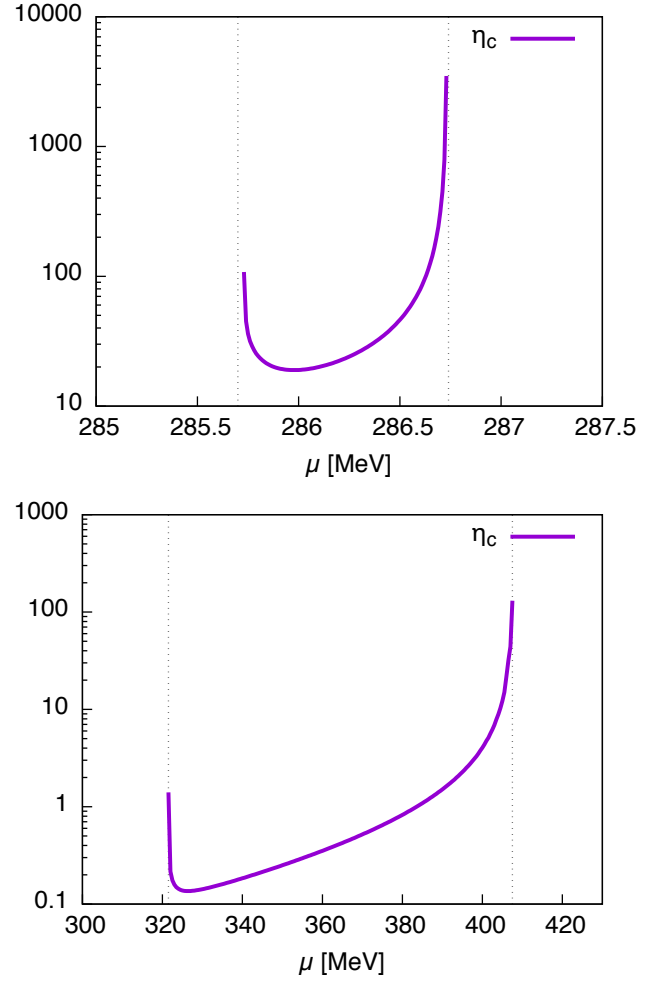


FIG. 6. The exponent η_c characterizing the algebraic decay of the order parameter correlation function in the kink crystal phase at $T = 70$ MeV (top) and $T = 10$ MeV (bottom). The dotted vertical lines mark the boundaries of the modulated phase.

parameter behaves for $|\mathbf{x}| \gg L$ as

$$\begin{aligned} \langle M(\mathbf{x})M(0) \rangle &= \sum_{n,m} \frac{\mathcal{M}_n \mathcal{M}_m}{L} e^{inQz} \langle \exp [iQ(nu(\mathbf{x}) + mu(\mathbf{0}))] \rangle \\ &= \sum_{n,m} \frac{\mathcal{M}_n \mathcal{M}_m}{L} e^{inQz} \exp \left[-\frac{Q^2}{2} \langle (nu(\mathbf{x}) + mu(\mathbf{0}))^2 \rangle \right] \\ &= \sum_{n,m} \frac{\mathcal{M}_n \mathcal{M}_m}{L} e^{inQz} \exp \left[-\frac{Q^2 T}{2} \int \frac{d^3k}{(2\pi)^3} \frac{m^2 + n^2 + 2mn e^{i\mathbf{k}\cdot\mathbf{x}}}{Bk_z^2 + Ck_\perp^4} \right] \\ &= \sum_{n,m} \frac{\mathcal{M}_n \mathcal{M}_m}{L} e^{inQz} \delta_{n,-m} \exp \left[-n^2 Q^2 T \int \frac{d^3k}{(2\pi)^3} \frac{1 - e^{i\mathbf{k}\cdot\mathbf{x}}}{Bk_z^2 + Ck_\perp^4} \right] \\ &\approx \sum_{n \geq 1} \frac{|\mathcal{M}_n|^2}{L} \begin{cases} 2 \cos(nQz) \times |z|^{-n^2 \eta_c} & (\mathbf{x}_\perp = \mathbf{0}) \\ |x_\perp|^{-2n^2 \eta_c} & (z = 0) \end{cases}. \end{aligned} \quad (27)$$

In the intermediate step, we have dropped terms with

$n \neq -m$ since their momentum integrals are infrared divergent. The exponent η_c above is defined by

$$\eta_c = \frac{Q^2 T}{8\pi\sqrt{BC}}, \quad (28)$$

which was originally introduced by Caillé [47]. Such an algebraic decay of the order parameter correlation has been known to appear in the smectic-A phase of liquid crystals [25, 31–33], in the FFLO phases of fermionic superfluids [34, 37, 38] and in the modulated pion condensation in nuclear matter [48]. Such a slow decay of the order parameter suggests that it would be hard in practice to distinguish it from a true long-range order.

In Fig. 6, we show the critical exponent η_c at $T = 70$ MeV and $T = 10$ MeV. Within numerical precision, η_c appears to go to infinity at the ends of the modulated phase. This is physically acceptable because an *exponential* decay of the connected two-point function is expected both in the symmetric phase and in the homogeneous broken phase.

Although $\langle M(\mathbf{x}) \rangle = 0$, a closer look at steps leading to (27) shows that $\langle M(\mathbf{x})^2 \rangle \neq 0$ in this phase. The real kink crystal phase is thus characterized by a homogeneous *higher-order condensate* consisting of four quarks, which is qualitatively distinct from the naive mean-field phase with $\langle M(\mathbf{x}) \rangle \neq 0$. These phases may be distinguished by $(\mathbb{Z}_2)_R \times (\mathbb{Z}_2)_L$ symmetry that flips signs of quarks of each chirality independently. Such a novel higher-order condensate is discussed for the FFLO phase of nonrelativistic fermions in [34, 37, 38].

The large fluctuation of phonons can be suppressed by several factors: (I) strictly zero temperature, (II) higher-dimensional modulations, (III) coupling to an external vector field (e.g., a magnetic field) and (IV) a finite volume. In case II, the phonon fluctuations no longer cause infrared singularity because the number of spatial directions with a quadratic dispersion decreases [25]. However, it is still an open problem whether higher-dimensional modulations can be energetically favored over a quasi-long-range-ordered phase. Case III is due to the fact that, as laid out in Appendix A, the explicit breaking of rotational invariance leads to a non-vanishing $(\nabla_\perp u)^2$ term. This leads to an interesting observation that inhomogeneous condensates in QCD under magnetic fields [49–53] could be stable against fluctuations.

Next, we shall analyze the finite-volume effect of case IV in detail. If the system size is finite, $\langle u^2 \rangle$ remains finite because the IR divergence is cut off. This is true for putative quark matter inside neutron stars. Roughly speaking, if $\langle u^2 \rangle < L^2$, the one-dimensional structure is expected to remain, while it is likely to be wiped out when $\langle u^2 \rangle > L^2$. Using (26), we define the crossover length ξ_\perp as a scale below which the one-dimensional modulation persists,

$$\xi_\perp = \sqrt{C/B} e^{4\pi L^2 \sqrt{BC}/T}, \quad (29)$$

which grows rapidly as the temperature decreases. The

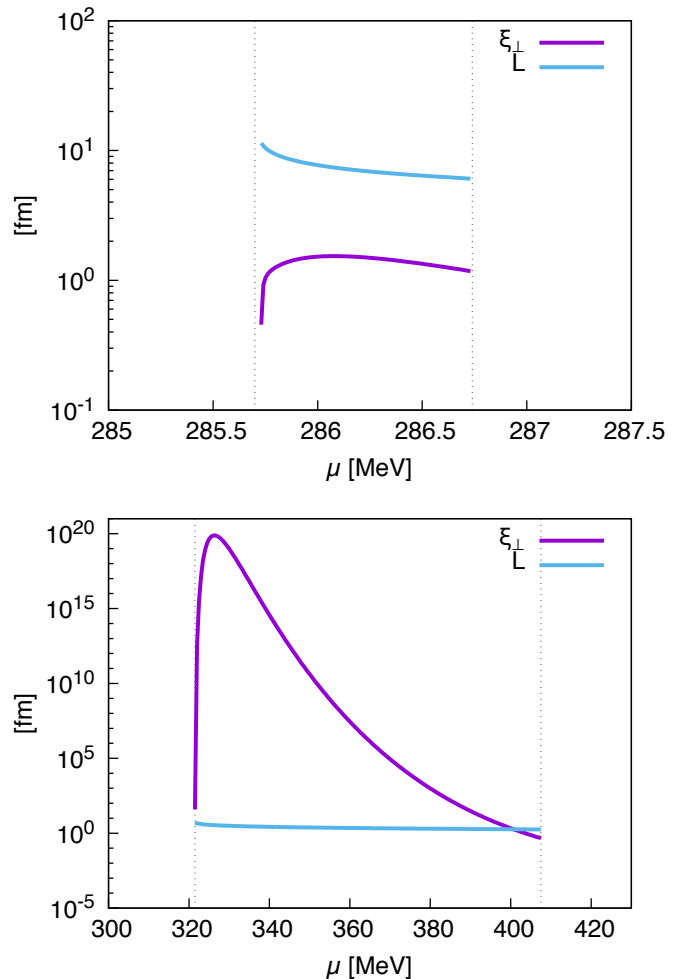


FIG. 7. The crossover scale ξ_\perp and the period L of the kink crystal at $T = 70$ MeV (top) and $T = 10$ MeV (bottom). The dotted vertical lines mark the boundaries of the modulated phase. Although $L \equiv 2\pi/Q$ diverges at the left boundary of the modulated phase (recall Fig. 2), this is not visible in these figures due to limited numerical precision.

periodic structure of the condensate will survive if the size ℓ of the quark matter is in the window $L \ll \ell \lesssim \xi_\perp$.

Figure 7 shows the crossover scale ξ_\perp together with the period L of the real kink crystal at $T = 70$ MeV and $T = 10$ MeV. It is observed that L is of order 1 fm throughout the modulated phase, while ξ_\perp has a strong T and μ -dependence. At high T , soft phonons are so easily excitable that the crossover length is comparable with the period. Thus, there is no vestige of a one-dimensional crystal at high temperature. On the other hand, at low T ($\lesssim 10$ MeV), the situation is different. As shown in the lower panel of Fig. 7, there is a region in which ξ_\perp is macroscopic, i.e., of order 1 km ($= 10^{18}$ fm), which would be presumably large enough to accommodate a quark core of neutron stars. Although the GL expansion is not quantitatively reliable at such a low temperature, our conclusion that the real kink crystal condensate persists

only at very low temperatures should be qualitatively correct.

D. Pions

Next we proceed to the analysis of gapless pions that stem from the spontaneous breaking of $SU(2)_R \times SU(2)_L$ to $SU(2)_V$. Unlike phonons that only emerge in the modulated phase, pions show up both in the homogeneous broken phase and in the real kink crystal phase, and hence it is of great interest to investigate the nature of pion fluctuations across the transition between these two phases. Since the vectorial isospin symmetry is intact in both phases we will only take account of the neutral pion fluctuation for simplicity, and defer a fuller analysis to Appendix B. As in [14, 15], let us make M complex as $M(\mathbf{x}) \equiv -2G[S(\mathbf{x}) + iP_3(\mathbf{x})]$, with $S(\mathbf{x}) = \langle \bar{\psi}\psi(\mathbf{x}) \rangle$ and $P_3(\mathbf{x}) = \langle \bar{\psi}i\gamma_5\tau^3\psi(\mathbf{x}) \rangle$. It has been shown by Nickel [14, 15] that, assuming a one-dimensional modulation, the (3 + 1)-dimensional GL Lagrangian for M can be obtained from that of the chiral Gross–Neveu model [22–24], leading to the result

$$\begin{aligned} \Omega_{\text{GL}}[M(\mathbf{x})] &= \alpha_2|M|^2 + \alpha_4\{|M|^4 + |\nabla M|^2\} \\ &\quad + \alpha_6\{2|M|^6 + 8|M|^2|\nabla M|^2 \\ &\quad + 2\text{Re}[(\nabla M)^2 M^{*2}] + |\Delta M|^2\}. \end{aligned} \quad (30)$$

Now we shall follow the same route as for phonons. In the following, π_0 will be denoted as π in order not to clutter notation. Substituting

$$M(\mathbf{x}) = M_0(z) e^{i\pi(\mathbf{x})} \quad (31)$$

into (5) and expanding in π , we obtain

$$\begin{aligned} \Omega_{\text{GL}}[M(\mathbf{x})] &= \Omega_{\text{GL}}[M_0(z)] + \frac{f_{1\pi}(z)}{2}(\partial_z\pi)^2 + \frac{f_{2\pi}(z)}{2}(\partial_z^2\pi)^2 \\ &\quad + \frac{g_{1\pi}(z)}{2}(\nabla_{\perp}\pi)^2 + \frac{g_{2\pi}(z)}{2}(\nabla_{\perp}^2\pi)^2 \\ &\quad + h_{1\pi}(z)(\partial_z\pi)(\nabla_{\perp}^2\pi) \\ &\quad + h_{2\pi}(z)(\partial_z^2\pi)(\nabla_{\perp}^2\pi) + \mathcal{O}(\pi^3), \end{aligned} \quad (32)$$

where $f_{1\pi}$, $f_{2\pi}$, $g_{1\pi}$, $g_{2\pi}$, $h_{1\pi}$, $h_{2\pi}$ are defined as

$$\begin{aligned} f_{1\pi}(z) &= 2(\alpha_4 + 6\alpha_6 M_0^2)(M_0)^2 \\ &\quad + 4\alpha_6\{2(M_0')^2 - M_0 M_0''\}, \\ f_{2\pi}(z) &= 2\alpha_6(M_0)^2, \\ g_{1\pi}(z) &= 2(\alpha_4 + 6\alpha_6 M_0^2)(M_0)^2 - 4\alpha_6 M_0 M_0'', \\ g_{2\pi}(z) &= 2\alpha_6(M_0)^2, \\ h_{1\pi}(z) &= 4\alpha_6 M_0 M_0', \quad h_{2\pi}(z) = 2\alpha_6(M_0)^2. \end{aligned} \quad (33)$$

We note that, unlike the phonon,

$$\oint g_{1\pi} \neq 0. \quad (34)$$

The eigenvalue E_{π} of pions may be derived from the eigenvalue equation

$$E_{\pi}\pi = \frac{\delta F[\pi]}{\delta\pi} \quad (35)$$

with

$$\begin{aligned} F[\pi] &\equiv \int d^3x \left\{ \frac{f_{1\pi}(z)}{2}(\partial_z\pi)^2 + \frac{f_{2\pi}(z)}{2}(\partial_z^2\pi)^2 \right. \\ &\quad + \frac{g_{1\pi}(z)}{2}(\nabla_{\perp}\pi)^2 + \frac{g_{2\pi}(z)}{2}(\nabla_{\perp}^2\pi)^2 \\ &\quad \left. + h_{1\pi}(z)(\partial_z\pi)(\nabla_{\perp}^2\pi) + h_{2\pi}(z)(\partial_z^2\pi)(\nabla_{\perp}^2\pi) \right\}. \end{aligned} \quad (36)$$

In a more explicit form, it reads

$$H_{\pi}\pi = E_{\pi}\pi \quad (37)$$

with

$$\begin{aligned} H_{\pi} &\equiv -\partial_z(f_{1\pi}\partial_z) + \partial_z^2(f_{2\pi}\partial_z^2) - g_{1\pi}\nabla_{\perp}^2 + g_{2\pi}\nabla_{\perp}^4 \\ &\quad - (\partial_z h_{1\pi})\nabla_{\perp}^2 + \nabla_{\perp}^2\{h_{2\pi}, \partial_z^2\}_+. \end{aligned} \quad (38)$$

Since the structure of (37) is identical to the case of phonons (20), one can apply the same techniques to solve it. On the basis of Bloch's theorem, π may be decomposed as

$$\pi(\mathbf{x}) = e^{i\mathbf{k}_{\perp}\cdot\mathbf{x}_{\perp}} e^{ik_z z} \phi(z), \quad (39)$$

for a crystal momentum k_z and transverse momenta k_{\perp} . $\phi(z)$ is a periodic function with period L . Substituting this decomposition, we arrive at an eigenvalue equation for ϕ , which can be solved with the same numerical methods as for phonons.

In Fig. 8, we show the eigenvalues E_{π} for varying k_z and k_{\perp} . To analyze the lowest eigenvalue $E_{\pi,0}$ (red curves in Fig. 8), we have used a variational method along the lines of Appendix E, which shows that the leading behavior of $E_{\pi,0}$ near $k_z = k_{\perp} = 0$ is given by

$$E_{\pi,0} \sim F_{\parallel}^2 k_z^2 + F_{\perp}^2 k_{\perp}^2, \quad (40)$$

where

$$F_{\perp}^2 \equiv \oint g_{1\pi} \quad (41)$$

and F_{\parallel}^2 is a positive function that has to be computed numerically. The elastic free energy of low-energy pions is therefore

$$F_{\text{el}}^{\pi} = \frac{1}{2} \int d^3x \left[F_{\parallel}^2 (\partial_z\pi)^2 + F_{\perp}^2 (\nabla_{\perp}\pi)^2 \right]. \quad (42)$$

Since $F_{\perp}^2 \neq 0$, pions on the real kink crystal have a linear dispersion in all directions, in contrast to phonons. Thus the thermal fluctuations of pions neither cause any infrared divergence nor destroy the long-range order.

F_{\perp}^2 and F_{\parallel}^2 at $T = 70$ MeV are shown in Fig. 9. In the homogeneous broken phase, the system is isotropic and $F_{\perp}^2 = F_{\parallel}^2$. In the kink crystal phase, the system is anisotropic and the coefficients no longer coincide. In our calculation, in the kink crystal phase, $F_{\parallel}^2 > F_{\perp}^2$ holds at any temperature and chemical potential.

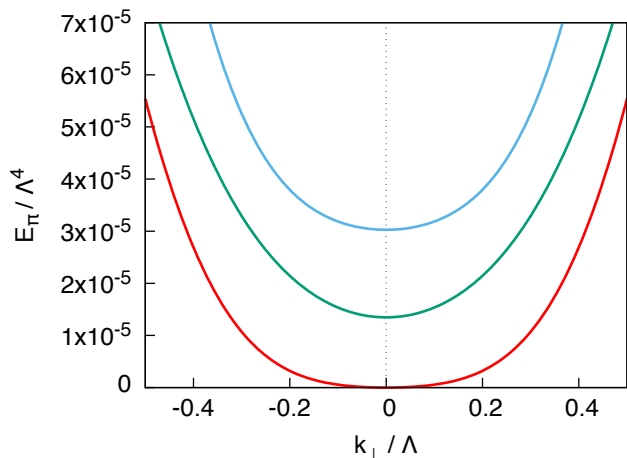
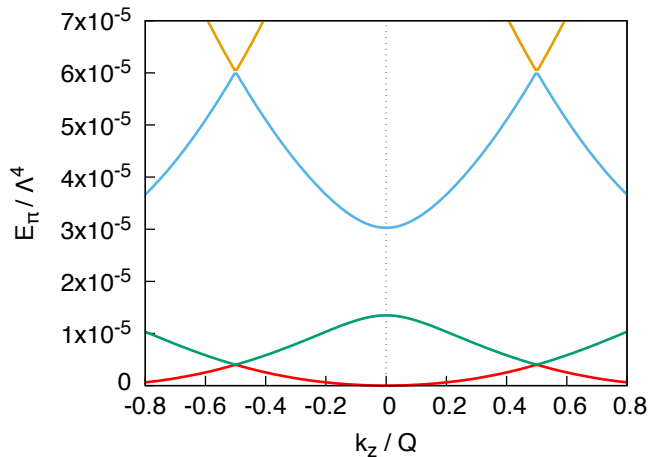


FIG. 8. Eigenvalues of H_π in (38) at $(T, \mu) = (70, 286.0)$ [MeV], for $k_\perp = 0$ (top) and for $k_z = 0$ (bottom). The domain $-0.5 \leq k_z/Q \leq 0.5$ is the first Brillouin zone. k_z and k_\perp are normalized by Q and Λ , respectively.

IV. CONCLUSION

In this paper, we presented a first systematic study of low-energy fluctuations in the real kink crystal phase of the NJL model. The elastic free energy for the phonon was shown to be $(\partial_z u)^2$ in the longitudinal direction and $(\partial_\perp^2 u)^2$ in the transverse directions with respect to the modulation of the condensate, which had an important consequence of vanishing order parameter, exhibiting a quasi-long-range order. We argued that, since the correlation function decays only algebraically, the real kink crystal may be sustained in compact star cores if the temperature is sufficiently low. Our analysis, which should be reliable at least near the critical point, suggests that fluctuation effects that are missed in the mean-field treatment change the nature of inhomogeneous chiral condensation qualitatively.

This work can be extended in various directions. The NJL model used here can be extended with the inclusion

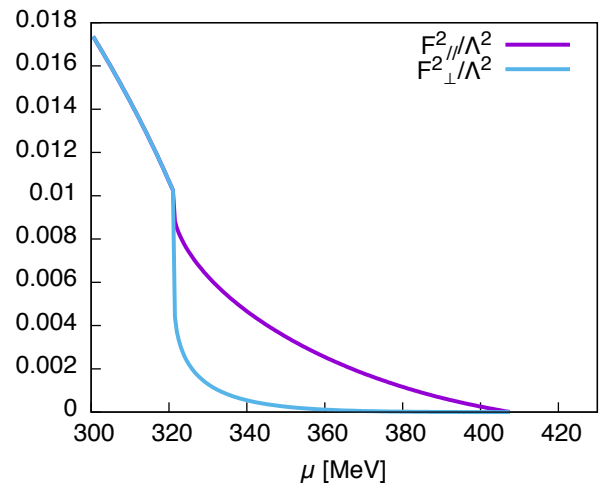
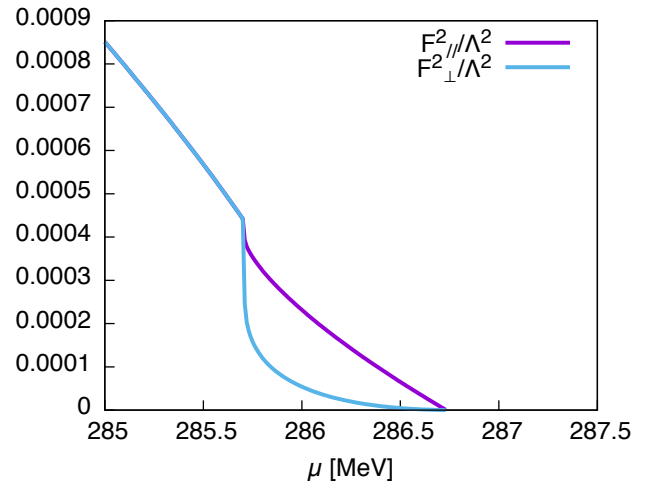


FIG. 9. F_\perp^2 and F_\parallel^2 at $T = 70$ MeV (top) and $T = 10$ MeV (bottom).

of vector interaction [16], or one can use the quark-meson model [15, 19]; in either case, the phase structure would be quantitatively modified. For a fuller understanding of the phonon fluctuation, we need to consider anharmonic effects due to the $\mathcal{O}(u^3)$ term in (4), which is known for the case of smectic liquid crystals to modify the scaling behavior (27) [54, 55]. It is also intriguing to study the interaction between quarks, phonons and pions. As for the fate of the Lifshitz critical point in Fig. 1, we point out that it must be eliminated from the QCD phase diagram once fluctuations are fully incorporated, because the lower critical dimension of the isotropic Lifshitz critical behavior with continuous symmetry is 4 [56]. This is true in the chiral limit, while for nonzero quark masses, the continuous symmetry is broken, and a more careful study is needed. At any rate, the mean-field picture can fail even qualitatively near the Lifshitz point, and it is highly desirable to develop a method for analyzing fluctuations that goes beyond the GL expansion. This is a hard problem at this stage but should be seriously considered in future research.

Finally we note that for phenomenological applications to the physics of compact stars it would be important to incorporate effects of nonzero quark masses, isospin chemical potential, electromagnetic interactions and color superconductivity, which deserves further investigation.

Note added

While this work was being completed, we learned of an independent work [57] where the low-energy fluctuations over a Fulde–Ferrell type inhomogeneous chiral condensate were discussed. That condensate breaks translational and internal symmetries in a different way from the real kink crystal considered in our work, and hence produces a different number of Nambu–Goldstone modes.

ACKNOWLEDGMENTS

We thank G. Baym, T.-G. Lee and D. A. Takahashi for useful discussions. K. K. and T. N. were supported by the Special Postdoctoral Research Program of RIKEN. Y. H. was supported by JSPS KAKENHI Grants No. 24740184. T. K. was supported by the RIKEN iTHES project.

Appendix A: Phonon effective theory coupled to a vector field

In this Appendix we present a simple argument based on the method of [44] showing that a coupling to an external vector field modifies the dispersion of phonons in a qualitative manner.

Let us start with a theory with no vector field. Suppose $\langle \phi \rangle = \phi_0(z)$ is a modulated static solution that minimizes the rotationally symmetric free energy $F[\phi] = \int d^3x \mathcal{F}(\phi, \partial\phi)$. Now we consider a translational fluctuation corresponding to the phonon around this solution, $\phi(\mathbf{x}) = \phi_0(z + u(\mathbf{x}))$. Plugging this into $F[\phi]$ and expanding in powers of u and ∇u , one obtains the effective theory for the u field. Since u always appears in the form, $z + u$, the effective free energy is constructed from

$$\text{scalar functions of } z + u, \text{ their derivatives, and } \delta_{ij}. \quad (\text{A1})$$

More concretely, the ingredients with one and two derivatives are

$$\partial_i(z + u) = \delta_i^z + \partial_i u, \quad (\text{A2})$$

$$\partial_i \partial_j(z + u) = \partial_i \partial_j u, \quad (\text{A3})$$

respectively. These ingredients are compatible with the original symmetry as they should be. For example,

$$(\delta_i^z + \partial_i u)^2 = 1 + 2\partial_z u + (\nabla u)^2 \quad (\text{A4})$$

automatically reproduces the rotationally invariant combination derived in Sec. II. It is now straightforward to

combine these ingredients and derive the leading phonon free energy

$$\mathcal{F} = A \left[\partial_z u + \frac{1}{2}(\nabla u)^2 \right] + B \left[\partial_z u + \frac{1}{2}(\nabla u)^2 \right]^2. \quad (\text{A5})$$

Just as we discussed in Sec. II, the total derivative term, $\partial_z u$, linear in u is prohibited by the minimum-energy condition, so that we have $A = 0$ and \mathcal{F} reduces to (4) after taking into account higher derivative terms. The reader is referred to [44] for more details of this method.

We shall then proceed to a discussion on the elastic free energy in the presence of an external vector field v^i . Such a situation is pertinent to modulated chiral condensates in QCD with an external magnetic field. Now one can use v^i in addition to the previous ingredients (A1), so that the following interaction can appear in the free energy for example:

$$v_i (\delta_i^z + \partial_i u) = v^z + v^i \partial_i u. \quad (\text{A6})$$

The simplest modification of (A5) will then be

$$\mathcal{F} = A \left[\partial_z u + \frac{1}{2}(\nabla u)^2 \right] + B \left[\partial_z u + \frac{1}{2}(\nabla u)^2 \right]^2 - v^z - v^i \partial_i u. \quad (\text{A7})$$

We notice here that the total derivative terms in the linear order arise from both of the A and v^i couplings. If the vector v_i is an external field, i.e., a non-dynamical field, and takes a value

$$v^i = A \delta_z^i, \quad (\text{A8})$$

the linear order terms cancel out:

$$\mathcal{F} = \frac{A}{2}(\nabla u)^2 + B(\partial_z u)^2 + \mathcal{O}(u^3). \quad (\text{A9})$$

Therefore, when an external field v^i explicitly breaks the rotation symmetry, the $(\nabla_{\perp} u)^2$ term need not vanish, which can be realized without spoiling the minimum-energy condition of the condensate. The dispersion of phonons becomes linear in all directions, implying that the severe infrared divergence at finite temperature (cf. Sec. III C) is ameliorated.

It would be important to note that the non-vanishing $(\nabla_{\perp} u)^2$ term in the free energy does not arise if the vector is *dynamical* (i.e., not external) and its condensation is aligned in the z -direction. In such a case, we have gapped fluctuations associated with the spontaneously broken rotational symmetries, just as in the smectic-A phase of liquid crystals. The free energy after integrating out those gapped fluctuations turns out to be the same as the one without dynamical vector fields, (4), which results in a strongly anisotropic dispersion of phonons.

Appendix B: GL expansion with pions

In this Appendix, we incorporate pionic modes into the effective theory (30) so that it becomes manifestly

invariant under $SU(2)_R \times SU(2)_L$. It is convenient to work with the matrix field

$$\Sigma(\mathbf{x}) \equiv -2G[S(\mathbf{x})\mathbb{1} + iP_a(\mathbf{x})\tau^a], \quad (\text{B1})$$

where $\{\tau^a\}$ are the Pauli matrices. Under $U_R \in SU(2)_R$ and $U_L \in SU(2)_L$, it transforms as $\Sigma \rightarrow U_L \Sigma U_R^\dagger$. Then the most generic GL function invariant under $SU(2)_R \times SU(2)_L$ is given, up to 6th order in fields and derivatives, by

$$\begin{aligned} \Omega_{\text{GL}}(\Sigma) = & \frac{\alpha_2}{2} \text{tr}[\Sigma^\dagger \Sigma] + \frac{\alpha_4}{2} \text{tr}[\partial_i \Sigma^\dagger \partial_i \Sigma] + \frac{\alpha_4}{4} (\text{tr}[\Sigma^\dagger \Sigma])^2 \\ & + \frac{\alpha_6}{4} (\text{tr}[\Sigma^\dagger \Sigma])^3 + \frac{\alpha_6}{2} \text{tr}[\Delta \Sigma^\dagger \Delta \Sigma] \\ & + \beta_1 \text{tr}[\Sigma^\dagger \Sigma] \text{tr}[\partial_i \Sigma^\dagger \partial_i \Sigma] \\ & + \beta_2 \{ \text{tr}[(\partial_i \Sigma) \Sigma^\dagger (\partial_i \Sigma) \Sigma^\dagger] + \text{h.c.} \} \\ & + \beta_3 (\text{tr}[\Sigma^\dagger \partial_i \Sigma])^2 + \beta_4 \text{tr}[\Sigma^\dagger \Sigma] \text{tr}[\Sigma^\dagger \Delta \Sigma], \end{aligned} \quad (\text{B2})$$

where the coefficients β_1 , β_2 , β_3 and β_4 are yet to be determined. However, the last four terms of (B2) are not independent, owing to the relations

$$\begin{aligned} & \text{tr}[(\partial_i \Sigma) \Sigma^\dagger (\partial_i \Sigma) \Sigma^\dagger] \\ & = (\text{tr}[\Sigma^\dagger \partial_i \Sigma])^2 - \frac{1}{2} \text{tr}[\Sigma^\dagger \Sigma] \text{tr}[\partial_i \Sigma^\dagger \partial_i \Sigma], \end{aligned} \quad (\text{B3})$$

and

$$\begin{aligned} & \text{tr}[\Sigma^\dagger \Sigma] \text{tr}[\Sigma^\dagger \Delta \Sigma] \\ & = \partial_i (\text{tr}[\Sigma^\dagger \Sigma] \text{tr}[\Sigma^\dagger \partial_i \Sigma]) - 2 (\text{tr}[\Sigma^\dagger \partial_i \Sigma])^2 \\ & \quad - \text{tr}[\Sigma^\dagger \Sigma] \text{tr}[\partial_i \Sigma^\dagger \partial_i \Sigma]. \end{aligned} \quad (\text{B4})$$

Therefore one can let $\beta_2 = \beta_4 = 0$ without loss of generality (up to total derivatives). Since $\Omega_{\text{GL}}(\Sigma)$ must reduce to (30) when $P_1 = P_2 = 0$, we require

$$\begin{aligned} & \alpha_6 \{ 8|M|^2 |\nabla M|^2 + 2 \text{Re} [(\nabla M)^2 M^{*2}] \} \stackrel{!}{=} \\ & 4\beta_1 |M|^2 |\nabla M|^2 + 2\beta_3 \{ |M|^2 |\nabla M|^2 + \text{Re} [(\nabla M)^2 M^{*2}] \}. \end{aligned}$$

$$\therefore \beta_1 = \frac{3}{2} \alpha_6 \quad \text{and} \quad \beta_3 = \alpha_6. \quad (\text{B5})$$

Thus the desired GL function with manifest chiral symmetry is given by

$$\begin{aligned} & \Omega_{\text{GL}}(\Sigma) \\ & = \frac{\alpha_2}{2} \text{tr}[\Sigma^\dagger \Sigma] + \frac{\alpha_4}{2} \text{tr}[\partial_i \Sigma^\dagger \partial_i \Sigma] + \frac{\alpha_4}{4} (\text{tr}[\Sigma^\dagger \Sigma])^2 \\ & \quad + \frac{\alpha_6}{4} (\text{tr}[\Sigma^\dagger \Sigma])^3 + \frac{\alpha_6}{2} \text{tr}[\Delta \Sigma^\dagger \Delta \Sigma] \\ & \quad + \frac{3\alpha_6}{2} \text{tr}[\Sigma^\dagger \Sigma] \text{tr}[\partial_i \Sigma^\dagger \partial_i \Sigma] + \alpha_6 (\text{tr}[\Sigma^\dagger \partial_i \Sigma])^2. \end{aligned} \quad (\text{B6})$$

Appendix C: Regularization of the thermodynamic potential

In the main body of this paper, we have employed the momentum cutoff to regularize UV divergences in the NJL model. Although the momentum cutoff is subtle in the presence of a modulated condensate as is claimed in [14, 20], our work is concerned with the GL expansion around a homogeneous vacuum, and so this problem is unlikely to obstruct our present analysis. We would also like to add that the phase structure including a modulated phase has been found to be quite robust against varying regularizations [58]. That being said, however, it would be desirable for theoretical completeness to have an alternative derivation of regularized GL coefficients that is free from the above subtlety. In this Appendix we shall demonstrate one of such regularization methods.

Let us start from the mean-field thermodynamic potential of the NJL model in Euclidean spacetime,

$$\begin{aligned} \Omega_{\text{MF}}(T, \mu) = & -N_c N_f \log \det [\not{\partial} - \mu \gamma_4 + M(\mathbf{x})] \\ & + \int d^4x \frac{M(\mathbf{x})^2}{4G}. \end{aligned} \quad (\text{C1})$$

The functional determinant suffers from UV divergences, and one has to specify a regularization scheme. The conventional three-momentum cutoff is not useful for a generic inhomogeneous mean field, whereas the Schwinger proper-time regularization [59] is tricky at nonzero chemical potential [60, 61]. Now we introduce a new regularization scheme free from these problems, based on the formula

$$\log A - \log B = - \int_0^\infty dw w \left\{ \frac{1}{(w+A)^2} - \frac{1}{(w+B)^2} \right\}. \quad (\text{C2})$$

See [62, 63] for the relation of this approach to the naive proper-time regularization. The methodology of derivative expansion is well known [64], and we shall be brief here,

$$\begin{aligned}
& \log \frac{\det[\not{\partial} - \mu\gamma_4 + M]}{\det[\not{\partial} - \mu\gamma_4]} = \frac{1}{2} \text{Tr} \left\{ \log [-(\partial_4 - \mu)^2 - \Delta + (\not{\nabla}M) + M^2] - \log [-(\partial_4 - \mu)^2 - \Delta] \right\} \\
& = -\frac{1}{2} \text{tr} \int_x \int_p \int_0^{\Lambda^2} dw w e^{-ipx} \left\{ \frac{1}{[w - (\partial_4 - \mu)^2 - \Delta + (\not{\nabla}M) + M^2]^2} - \frac{1}{[w - (\partial_4 - \mu)^2 - \Delta]^2} \right\} e^{ipx} \\
& = -\frac{1}{2} \text{tr} \int_x \int_p \int_0^{\Lambda^2} dw w \left\{ \frac{1}{[w + (p_4 + i\mu)^2 - (\nabla + i\mathbf{p})^2 + (\not{\nabla}M) + M^2]^2} - \frac{1}{[w + (p_4 + i\mu)^2 + \mathbf{p}^2]^2} \right\} \\
& = \frac{1}{2} \int_x \int_p \int_0^{\Lambda^2} dw \left\{ \frac{2w}{(w + P^2)^3} \text{tr} \hat{O} - \frac{3w}{(w + P^2)^4} \text{tr} \hat{O}^2 + \frac{4w}{(w + P^2)^5} \text{tr} \hat{O}^3 - \frac{5w}{(w + P^2)^6} \text{tr} \hat{O}^4 + \dots \right\},
\end{aligned}$$

where the “tr” denotes a trace over spinor indices, Λ is a UV cutoff, $\int_x \equiv \int d^4x$, $\int_p \equiv T \sum_{p_4} \int \frac{d^3p}{(2\pi)^3}$, $\hat{O} \equiv -2i\mathbf{p} \cdot \nabla - \Delta + (\not{\nabla}M) + M^2$ and $P^2 \equiv (p_4 + i\mu)^2 + \mathbf{p}^2$. For the purpose of obtaining the GL expansion up to 6th order, it suffices to expand only up to \hat{O}^4 . After a bit of algebra involving a trick $p_i p_j \rightarrow \delta_{ij} \mathbf{p}^2/3$ and integration by parts, we obtain

$$\begin{aligned}
\text{tr} \hat{O} &= 4M^2, \\
\text{tr} \hat{O}^2 &= 4[(\nabla M)^2 + M^4], \\
\text{tr} \hat{O}^3 &= 4[M^6 + 7M^2(\nabla M)^2 + (\Delta M)^2], \\
\text{tr} \hat{O}^4 &= \frac{16}{3} \mathbf{p}^2 [4M^2(\nabla M)^2 + (\Delta M)^2],
\end{aligned} \tag{C3}$$

where we have omitted total derivatives, terms that are higher order in the GL expansion, and terms odd in \mathbf{p} . Using a formula $\int_p \frac{\mathbf{p}^2}{(w+P^2)^6} = \frac{3}{10} \int_p \frac{1}{(w+P^2)^5}$, we can match the expanded determinant with (5) and extract the regularized GL coefficients as

$$\alpha_2 = \frac{1}{4G} - 4N_c N_f \int_p \int_0^{\Lambda^2} dw \frac{w}{(w + P^2)^3}, \tag{C4a}$$

$$\alpha_4 = 6N_c N_f \int_p \int_0^{\Lambda^2} dw \frac{w}{(w + P^2)^4}, \tag{C4b}$$

$$\alpha_6 = -4N_c N_f \int_p \int_0^{\Lambda^2} dw \frac{w}{(w + P^2)^5}. \tag{C4c}$$

In the limit $\Lambda \rightarrow \infty$, we formally recover (6). This derivation, in which the functional determinant is regularized directly, satisfies the requirement [14, 20] that surface terms in momentum integrals strictly vanish. However, the three-momentum cutoff is practically more useful and is used throughout the main part of this paper.

Appendix D: Proof of $\oint g_1 = 0$

In this Appendix, we prove (17), i.e., that $g_1(z)$ must vanish in the average sense when ν and q in (8) are so

tuned that $M_0(z)$ attains the minimum of the free energy per period. To show this, we consider a scaled configuration

$$M(\lambda, z) \equiv M_0(\lambda z), \tag{D1}$$

which has a period L/λ with L defined in (10). It follows from the minimum-energy requirement for $M_0(z)$ that the GL free energy per period of $M(\lambda, z)$ must have an extremum at $\lambda = 1$, namely

$$\lim_{\lambda \rightarrow 1} \frac{\partial}{\partial \lambda} \left[\frac{1}{L/\lambda} \int_0^{L/\lambda} dz \Omega_{\text{GL}}[M(\lambda, z)] \right] = 0. \tag{D2}$$

Note that this equality is trivial if $\Omega_{\text{GL}}[M]$ did not depend on the derivatives of M , for one can simply get rid of λ from inside of $[\dots]$ via a change of variable $z \rightarrow z/\lambda$. However, this is not possible for $\Omega[M]$ in (5) which does depend on the derivatives of M .

An explicit calculation yields

$$\frac{\partial}{\partial \lambda} \left[\frac{1}{L/\lambda} \int_0^{L/\lambda} dz \Omega_{\text{GL}}[M(\lambda, z)] \right] = \boxed{1} + \boxed{2} + \boxed{3}, \tag{D3}$$

where [with $M' \equiv \partial_z M(\lambda, z)$ and $M'' \equiv \partial_z^2 M(\lambda, z)$, and

omitting the subscript ‘‘GL’’ for brevity]

$$\boxed{1} = \frac{1}{L} \int_0^{L/\lambda} dz \Omega[M(\lambda, z)], \quad (\text{D4})$$

$$\boxed{2} = -\frac{1}{\lambda} \Omega[M(\lambda, L/\lambda)] = -\frac{1}{\lambda} \Omega[M_0(L)], \quad (\text{D5})$$

$$\begin{aligned} \boxed{3} &= \frac{1}{L/\lambda} \int_0^{L/\lambda} dz \frac{\partial}{\partial \lambda} \Omega[M(\lambda, z)] \quad (\text{D6}) \\ &= \frac{1}{L/\lambda} \int_0^{L/\lambda} dz \left(\frac{\partial \Omega}{\partial M} + \frac{\partial \Omega}{\partial M'} \partial_z + \frac{\partial \Omega}{\partial M''} \partial_z^2 \right) \frac{\partial M}{\partial \lambda} \quad (\text{D7}) \end{aligned}$$

$$\begin{aligned} &= \frac{1}{L} \int_0^{L/\lambda} dz \left[z \left(\frac{\partial \Omega}{\partial M} M' + \frac{\partial \Omega}{\partial M'} M'' + \frac{\partial \Omega}{\partial M''} M''' \right) \right. \\ &\quad \left. + \frac{\partial \Omega}{\partial M'} M' + 2 \frac{\partial \Omega}{\partial M''} M'' \right] \quad (\text{D8}) \end{aligned}$$

$$= \frac{1}{L} \int_0^{L/\lambda} dz \left[z \frac{d\Omega}{dz} + \frac{\partial \Omega}{\partial M'} M' + 2 \frac{\partial \Omega}{\partial M''} M'' \right] \quad (\text{D9})$$

$$\begin{aligned} &= \frac{1}{\lambda} \Omega[M_0(L)] - \frac{1}{L} \int_0^{L/\lambda} dz \Omega[M] \\ &\quad + \frac{1}{L} \int_0^{L/\lambda} dz \left[\frac{\partial \Omega}{\partial M'} M' + 2 \frac{\partial \Omega}{\partial M''} M'' \right]. \quad (\text{D10}) \end{aligned}$$

In the step from (D7) to (D8), we used the relation $\frac{\partial M}{\partial \lambda} = \frac{z}{\lambda} M'$. Now, plugging $\boxed{1}$, $\boxed{2}$ and $\boxed{3}$ into (D3) and taking the limit $\lambda \rightarrow 1$, we obtain

$$\oint \left[\frac{\partial \Omega}{\partial M'} M' + 2 \frac{\partial \Omega}{\partial M''} M'' \right] \Big|_{M=M_0} = 0. \quad (\text{D11})$$

Recalling that $\Omega_{\text{GL}}[M]$ is given by (5), this translates into

$$\oint [2(\alpha_4 + 10\alpha_6 M_0^2)(M_0')^2 + 4\alpha_6 (M_0'')^2] = 0, \quad (\text{D12})$$

which reduces to $\oint g_1 = 0$ via integration by parts. This completes the proof. We stress that the stability of the condensate under dilatation has played an essential role here.

Appendix E: Variational analysis for the lowest eigenvalue spectrum of phonons

In this Appendix we apply a variational technique to the eigenvalue problem (20) and show that the energy of

long-wavelength phonons is given, at leading order, by (23). First of all, we note that, among infinitely many energy levels that follow from (23), it is only the lowest level E_0 that matters for the low-energy phonons. Then it is easily seen that E_0 for given $k = (k_\perp, k_z)$ is given by the formula

$$\begin{aligned} E_0(k) &= \min_{u \in \mathfrak{U}(k)} \frac{1}{\oint |u|^2} \oint \left\{ f_1 |\partial_z u|^2 + f_2 |\partial_z^2 u|^2 \right. \\ &\quad \left. + (g_1 + \partial_z h_1) |\nabla_\perp u|^2 + g_2 |\nabla_\perp^2 u|^2 \right. \\ &\quad \left. + h_2 (\partial_z^2 \bar{u})(\nabla_\perp^2 u) + h_2 (\nabla_\perp^2 \bar{u})(\partial_z^2 u) \right\}, \quad (\text{E1}) \end{aligned}$$

where $\mathfrak{U}(k)$ stands for the set of smooth functions of the form

$$\begin{aligned} u(\mathbf{x}) &= e^{ik_z z} e^{i\mathbf{k}_\perp \cdot \mathbf{x}_\perp} \phi(z), \quad (\text{E2}) \\ \phi(z+L) &= \phi(z), \quad k_z, k_\perp \in \mathbb{R}. \end{aligned}$$

1. Eigenvalue with $k_\perp \neq 0$ and $k_z = 0$

Now we consider E_0 for nonzero transverse momenta. Substituting (E2) with $k_z = 0$ into (E1), we get

$$\begin{aligned} E_0(k_\perp) &= \min_\phi \frac{1}{\oint |\phi|^2} \oint \left[f_1 |\phi'|^2 + f_2 |\phi''|^2 \right. \\ &\quad \left. + (k_\perp^2 \tilde{g}_1 + k_\perp^4 g_2) |\phi|^2 - k_\perp^2 h_2 (\overline{\phi''} \phi + \overline{\phi} \phi'') \right], \quad (\text{E3}) \end{aligned}$$

where the primes denote derivatives by z and we defined $\tilde{g}_1 \equiv g_1 + h_1'$. When $k_\perp = 0$, the minimum is trivially $E_0 = 0$, which is achieved by an arbitrary constant solution: $\phi(z) = \phi_0 \neq 0$. Now for sufficiently small k_\perp , we can expand ϕ that corresponds to the minimum of (E3) in perturbative series of k_\perp as

$$\phi(z) = \phi_0 [1 + k_\perp \phi_1(z) + k_\perp^2 \phi_2(z) + \dots]. \quad (\text{E4})$$

Plugging this into (E3) yields

$$\begin{aligned} E_0(k_\perp) &= \min_\phi \{ \beta_2 [\phi_1] k_\perp^2 + \beta_3 [\phi_1] k_\perp^3 + \beta_4 [\phi_1] k_\perp^4 + \mathcal{O}(k_\perp^5) \} \\ &\equiv \beta_{2*} k_\perp^2 + \beta_{3*} k_\perp^3 + \beta_{4*} k_\perp^4 + \mathcal{O}(k_\perp^5), \quad (\text{E5}) \end{aligned}$$

with

$$\beta_2[\phi_1] = \oint \{f_1|\phi_1'|^2 + f_2|\phi_1''|^2 + \tilde{g}_1\}, \quad (\text{E6})$$

$$\beta_3[\phi_i] = \oint \{f_1(\overline{\phi_2}'\phi_1' + \overline{\phi_1}'\phi_2') + f_2(\overline{\phi_2}''\phi_1'' + \overline{\phi_1}''\phi_2'') + \tilde{g}_1(\phi_1 + \overline{\phi_1}) - h_2(\overline{\phi_1}'' + \phi_1'')\} - \beta_2[\phi] \oint (\phi_1 + \overline{\phi_1}), \quad (\text{E7})$$

$$\begin{aligned} \beta_4[\phi_i] = \oint \{f_1(|\phi_2'|^2 + \overline{\phi_1}'\phi_3' + \overline{\phi_3}'\phi_1') + f_2(|\phi_2''|^2 + \overline{\phi_1}''\phi_3'' + \overline{\phi_3}''\phi_1'') + \tilde{g}_1(|\phi_1|^2 + \phi_2 + \overline{\phi_2}) + g_2 \\ - h_2(\overline{\phi_1}''\phi_1 + \overline{\phi_1}'\phi_1' + \overline{\phi_2}'' + \phi_2'')\} - \beta_2[\phi] \oint (|\phi_1|^2 + \phi_2 + \overline{\phi_2}) - \beta_3[\phi] \oint (\phi_1 + \overline{\phi_1}). \end{aligned} \quad (\text{E8})$$

Since $E_0(k_\perp)$ is the minimal eigenvalue, the leading coefficient β_{2*} must be at the minimum as a functional of ϕ , i.e.,

$$\beta_{2*} = \min_{\phi_1} \oint \{f_1|\phi_1'|^2 + f_2|\phi_1''|^2 + \tilde{g}_1\}. \quad (\text{E9})$$

As f_1 and f_2 are positive functions, the minimum trivially occurs when $\phi_1' = 0$. Thus,

$$\beta_{2*} = \oint \tilde{g}_1 = \oint g_1 = 0, \quad (\text{E10})$$

where the last equality is proved in Appendix D.

Next substituting the solution $\phi_1' = 0$ into $\beta_3[\phi_i]$, we readily find that the coefficient of k_\perp^3 vanishes:

$$\beta_{3*} = \min_{\phi_1 \in \mathbb{C}} \left\{ \oint \{\tilde{g}_1(\phi_1 + \overline{\phi_1})\} - \beta_{2*} \oint (\phi_1 + \overline{\phi_1}) \right\} = 0. \quad (\text{E11})$$

Finally we come to the coefficient of k_\perp^4 . Since it is the leading nonzero term in $E_0(k_\perp)$, it must be minimized as a functional of ϕ . Substituting $\phi_1' = 0$ into $\beta_4[\phi_i]$ and using $\beta_{2*} = \beta_{3*} = 0$, we obtain

$$\begin{aligned} \beta_{4*} = \oint g_2 + \min_{\phi_2} \oint \{f_1|\phi_2'|^2 + f_2|\phi_2''|^2 \\ + \tilde{g}_1(\phi_2 + \overline{\phi_2}) - h_2(\overline{\phi_2}'' + \phi_2'')\}. \end{aligned} \quad (\text{E12})$$

Although it is not analytically tractable, one can in principle determine ϕ_2 that minimizes the integral by solving the Euler-Lagrange equation

$$-(f_1\phi_2')' + (f_2\phi_2'')'' + \tilde{g}_1 - h_2'' = 0 \quad (\text{E13})$$

with periodic boundary conditions.

Summarizing above, the eigenvalue E_0 for transverse momenta is given by

$$E_0(k_\perp) = \beta_{4*}k_\perp^4 + \mathcal{O}(k_\perp^5). \quad (\text{E14})$$

2. Eigenvalue spectrum with $k_z \neq 0$ and $k_\perp = 0$

Next we consider E_0 for parallel direction,

$$\begin{aligned} E_0(k_z) \\ = \min_{\phi} \frac{\oint \{f_1|ik_z\phi + \phi'|^2 + f_2|k_z^2\phi - 2ik_z\phi' - \phi''|^2\}}{\oint |\phi|^2}. \end{aligned} \quad (\text{E15})$$

When $k_z = 0$, the minimum is trivially $E_0 = 0$, corresponding to a constant solution $\phi(z) = \phi_0 \neq 0$. Now, for sufficiently small k_z , one can expand ϕ that achieves the minimum of (E15) in a perturbative series of k_z as

$$\phi(z) = \phi_0[1 + k_z\chi_1(z) + k_z^2\chi_2(z) + \dots]. \quad (\text{E16})$$

Substituting this expansion, we find

$$E_0(k_z) = \min_{\phi} \{\gamma_2[\chi_1]k_z^2 + \mathcal{O}(k_z^3)\}, \quad (\text{E17})$$

with

$$\gamma_2[\phi_1] \equiv \oint \{f_1|1 - i\chi_1'|^2 + f_2|\chi_1''|^2\}. \quad (\text{E18})$$

Since $E_0(k_z)$ is the minimal eigenvalue, χ_1 must be chosen so as to minimize $\gamma_2[\chi_1]$. Thus, χ_1 satisfies the Euler-Lagrange equation

$$\frac{\delta\gamma_2[\chi_1]}{\delta\chi_1} = -if_1' - (f_1\chi_1')' + (f_2\chi_1'')'' = 0, \quad (\text{E19})$$

with periodic boundary conditions. Using the solution χ_{1*} , the eigenvalue at small k_z is finally obtained as

$$E_0(k_z) = \gamma_{2*}k_z^2 + \mathcal{O}(k_z^3), \quad (\text{E20})$$

with $\gamma_{2*} \equiv \gamma_2[\chi_{1*}]$.

3. Absence of $k_z k_\perp^2$ term in E_0

We have shown the leading behavior of E_0 for $k_\perp \neq 0$, $k_z = 0$, and for $k_\perp \neq 0, k_z = 0$ in the previous subsections. Here we show that E_0 does not have a $k_z k_\perp^2$ term, when both k_z and k_\perp are nonzero.

Since H_u in (21) is invariant under $z \rightarrow -z$, the eigenvalues with the momentum k_z and $-k_z$ degenerate, which implies the absence of the $k_z k_\perp^2$ term. To see this explicitly, let us decompose H_u into an unperturbed part H_0 and a perturbation V :

$$H_0 \equiv -\partial_z(f_1\partial_z) + \partial_z^2(f_2\partial_z^2), \quad (\text{E21})$$

$$V \equiv -g_1\nabla_\perp^2 + g_2\nabla_\perp^4 - (\partial_z h_1)\nabla_\perp^2 + \nabla_\perp^2 \{h_2, \partial_z^2\}_+ . \quad (\text{E22})$$

The lowest eigenvalue state for the unperturbed part can be expanded as

$$u(\mathbf{x}) = e^{ik_z z} e^{i\mathbf{k}_\perp \cdot \mathbf{x}_\perp} \phi_0 [1 + k_z \chi_1 + k_z^2 \chi_2 + \dots], \quad (\text{E23})$$

where χ_1 satisfies (E19). Since f_1 and f_2 are invariant under $z \rightarrow L - z$, the solution of (E19), $\chi_1(z)$, is an odd function, $\chi_1(L - z) = -\chi_1(z)$. Due to the periodic boundary condition, $\chi_1(0) = \chi_1(L) = 0$.

The eigenvalue for the unperturbed part is obtained as

$$E_0(k_z) = \frac{1}{\oint |u|^2} \oint \bar{u} H_0 u = \gamma_{2*} k_z^2 + \mathcal{O}(k_z^3). \quad (\text{E24})$$

Since V is of order ∇_\perp^2 , i.e., k_\perp^2 in momentum space, the first-order correction δE_0 gives the contribution of order k_\perp^2 , which is given by the expectation value of V for u :

$$\begin{aligned} \delta E_0 &= \frac{1}{\oint |u|^2} \oint \bar{u} V u \\ &= k_z k_\perp^2 \oint \left\{ \tilde{g}_1 (\chi_1 + \bar{\chi}_1) - h_2 (\chi_1'' + \bar{\chi}_1'') \right\} + \mathcal{O}(k_z^2 k_\perp^2). \end{aligned} \quad (\text{E25})$$

In the second line, we used (E10) and integration by parts. The integrand is odd under $z \rightarrow L - z$ because $\chi_1(L - z) = -\chi_1(z)$, $\tilde{g}_1(L - z) = \tilde{g}_1(z)$ and $h_2(L - z) = h_2(z)$. Therefore, the integral in the second line of (E25) vanishes, which proves the absence of the $k_z k_\perp^2$ term in E_0 .

-
- [1] M. G. Alford, A. Schmitt, K. Rajagopal, and T. Schäfer, *Rev. Mod. Phys.* **80**, 1455 (2008), arXiv:0709.4635 [hep-ph].
- [2] E. Shuryak, *Prog. Part. Nucl. Phys.* **62**, 48 (2009), arXiv:0807.3033 [hep-ph].
- [3] K. Fukushima and T. Hatsuda, *Rept. Prog. Phys.* **74**, 014001 (2011), arXiv:1005.4814 [hep-ph].
- [4] A. B. Migdal, *Rev. Mod. Phys.* **50**, 107 (1978).
- [5] D. Deryagin, D. Y. Grigoriev, and V. Rubakov, *Int. J. Mod. Phys. A* **7**, 659 (1992).
- [6] E. Shuster and D. Son, *Nucl. Phys. B* **573**, 434 (2000), arXiv:hep-ph/9905448 [hep-ph].
- [7] E. Nakano and T. Tatsumi, *Phys. Rev. D* **71**, 114006 (2005), arXiv:hep-ph/0411350 [hep-ph].
- [8] T. Kojo, Y. Hidaka, L. McLerran, and R. D. Pisarski, *Nucl. Phys. A* **843**, 37 (2010), arXiv:0912.3800 [hep-ph].
- [9] T. Kojo, Y. Hidaka, K. Fukushima, L. D. McLerran, and R. D. Pisarski, *Nucl. Phys. A* **875**, 94 (2012), arXiv:1107.2124 [hep-ph].
- [10] R. Casalbuoni and G. Nardulli, *Rev. Mod. Phys.* **76**, 263 (2004), arXiv:hep-ph/0305069 [hep-ph].
- [11] R. Anglani, R. Casalbuoni, M. Ciminale, N. Ippolito, R. Gatto, *et al.*, *Rev. Mod. Phys.* **86**, 509 (2014), arXiv:1302.4264 [hep-ph].
- [12] P. Fulde and R. A. Ferrell, *Phys. Rev.* **135**, A550 (1964).
- [13] A. Larkin and Y. N. Ovchinnikov, *Zh. Eksperim. i Teor. Fiz.* **47**, 1136 (1964).
- [14] D. Nickel, *Phys. Rev. Lett.* **103**, 072301 (2009), arXiv:0902.1778 [hep-ph].
- [15] D. Nickel, *Phys. Rev. D* **80**, 074025 (2009), arXiv:0906.5295 [hep-ph].
- [16] S. Carignano, D. Nickel, and M. Buballa, *Phys. Rev. D* **82**, 054009 (2010), arXiv:1007.1397 [hep-ph].
- [17] H. Abuki, D. Ishibashi, and K. Suzuki, *Phys. Rev. D* **85**, 074002 (2012), arXiv:1109.1615 [hep-ph].
- [18] S. Carignano and M. Buballa, *Phys. Rev. D* **86**, 074018 (2012), arXiv:1203.5343 [hep-ph].
- [19] S. Carignano, M. Buballa, and B.-J. Schaefer, *Phys. Rev. D* **90**, 014033 (2014), arXiv:1404.0057 [hep-ph].
- [20] M. Buballa and S. Carignano, *Prog. Part. Nucl. Phys.* **81**, 39 (2015), arXiv:1406.1367 [hep-ph].
- [21] M. Thies, *J. Phys. A* **39**, 12707 (2006), arXiv:hep-th/0601049 [hep-th].
- [22] G. Basar and G. V. Dunne, *Phys. Rev. Lett.* **100**, 200404 (2008), arXiv:0803.1501 [hep-th].
- [23] G. Basar and G. V. Dunne, *Phys. Rev. D* **78**, 065022 (2008), arXiv:0806.2659 [hep-th].
- [24] G. Basar, G. V. Dunne, and M. Thies, *Phys. Rev. D* **79**, 105012 (2009), arXiv:0903.1868 [hep-th].
- [25] L. D. Landau and E. Lifshitz, *Statistical physics* (Elsevier Science, 1996).
- [26] R. Peierls, *Helv. Phys. Acta* **7**, 81 (1934).
- [27] N. Mermin and H. Wagner, *Phys. Rev. Lett.* **17**, 1133 (1966).
- [28] S. R. Coleman, *Commun. Math. Phys.* **31**, 259 (1973).
- [29] V. Berezinskii, *Sov. Phys. JETP* **32**, 493 (1971).
- [30] J. M. Kosterlitz and D. J. Thouless, *J. Phys. C* **6**, 1181 (1973).
- [31] P.-G. De Gennes and J. Prost, *The physics of liquid crystals*, Vol. 23 (Clarendon press Oxford, 1993).
- [32] P. M. Chaikin and T. C. Lubensky, *Principles of condensed matter physics* (Cambridge Univ Press, 2000).
- [33] W. H. de Jeu, B. I. Ostrovskii, and A. N. Shalaginov, *Rev. Mod. Phys.* **75**, 181 (2003).
- [34] L. Radzihovsky and A. Vishwanath, *Phys. Rev. Lett.* **103**, 010404 (2008), arXiv:0812.3945 [cond-mat].
- [35] K. V. Samokhin, *Phys. Rev. B* **81**, 224507 (2010), arXiv:1003.2194 [cond-mat].
- [36] K. Samokhin, *Phys. Rev. B* **83**, 094514 (2011).
- [37] L. Radzihovsky, *Phys. Rev. A* **84**, 023611 (2011), arXiv:1102.4903 [cond-mat].
- [38] L. Radzihovsky, *Physica C: Superconductivity* **481**, 189 (2012), arXiv:1112.0773 [cond-mat].
- [39] J. P. A. Devreese and J. Tempere, *Phys. Rev. A* **89**,

- 013616 (2014), [arXiv:1310.3840 \[cond-mat\]](#).
- [40] I. Low and A. V. Manohar, *Phys. Rev. Lett.* **88**, 101602 (2002), [arXiv:hep-th/0110285](#).
- [41] H. Watanabe and H. Murayama, *Phys. Rev. Lett.* **110**, 181601 (2013), [arXiv:1302.4800 \[cond-mat.other\]](#).
- [42] T. Hayata and Y. Hidaka, *Phys. Lett.* **B735**, 195 (2014), [arXiv:1312.0008 \[hep-th\]](#).
- [43] H. Leutwyler, *Helv. Phys. Acta* **70**, 275 (1997), [arXiv:hep-ph/9609466 \[hep-ph\]](#).
- [44] Y. Hidaka, T. Noumi, and G. Shiu, (2014), [arXiv:1412.5601 \[hep-th\]](#).
- [45] D. A. Takahashi, (2013), [arXiv:1304.7567 \[cond-mat\]](#).
- [46] T. Hatsuda and T. Kunihiro, *Phys. Rept.* **247**, 221 (1994), [arXiv:hep-ph/9401310 \[hep-ph\]](#).
- [47] A. Caillé, *C. R. Seances Acad. Sci., Serie B* **274**, 891 (1972).
- [48] G. Baym, B. Friman, and G. Grinstein, *Nucl. Phys.* **B210**, 193 (1982).
- [49] D. Son and M. Stephanov, *Phys. Rev. D* **77**, 014021 (2008), [arXiv:0710.1084 \[hep-ph\]](#).
- [50] G. Basar, G. V. Dunne, and D. E. Kharzeev, *Phys. Rev. Lett.* **104**, 232301 (2010), [arXiv:1003.3464 \[hep-ph\]](#).
- [51] I. Frolov, V. C. Zhukovsky, and K. Klimenko, *Phys. Rev. D* **82**, 076002 (2010), [arXiv:1007.2984 \[hep-ph\]](#).
- [52] M. Eto, K. Hashimoto, and T. Hatsuda, *Phys. Rev. D* **88**, 081701 (2013), [arXiv:1209.4814 \[hep-ph\]](#).
- [53] T. Tatsumi, K. Nishiyama, and S. Karasawa, *Phys. Lett.* **B743**, 66 (2015), [arXiv:1405.2155 \[hep-ph\]](#).
- [54] G. Grinstein and R. A. Pelcovits, *Phys. Rev. Lett.* **47**, 856 (1981).
- [55] G. Grinstein and R. A. Pelcovits, *Phys. Rev. A* **26**, 915 (1982).
- [56] H. W. Diehl, *Acta physica slovacica* **52** (4), 271 (2002), [arXiv:cond-mat/0205284](#).
- [57] T.-G. Lee, E. Nakano, Y. Tsue, T. Tatsumi, and B. Friman, (2015), [arXiv:1504.03185 \[hep-ph\]](#).
- [58] T. L. Partyka and M. Sadzikowski, *J. Phys.* **G36**, 025004 (2009), [arXiv:0811.4616 \[hep-ph\]](#).
- [59] J. S. Schwinger, *Phys. Rev.* **82**, 664 (1951).
- [60] T. Inagaki, D. Kimura, and T. Murata, *Int. J. Mod. Phys.* **A20**, 4995 (2005), [arXiv:hep-ph/0307289 \[hep-ph\]](#).
- [61] H. Kohyama, D. Kimura, and T. Inagaki, *Nucl. Phys.* **B896**, 682 (2015), [arXiv:1501.00449 \[hep-ph\]](#).
- [62] D. F. Litim and J. M. Pawłowski, *Phys. Rev. D* **65**, 081701 (2002), [arXiv:hep-th/0111191 \[hep-th\]](#).
- [63] D. F. Litim and J. M. Pawłowski, *Phys. Rev. D* **66**, 025030 (2002), [arXiv:hep-th/0202188 \[hep-th\]](#).
- [64] T. Eguchi, *Phys. Rev. D* **14**, 2755 (1976).